Generation of Inner Ear Sensory Neurons Using Blastocyst Complementation in a *Neurog1*$^{+/-}$ - Deficient Mouse

Aleta R. Steevens (asteeven@umn.edu)
University of Minnesota https://orcid.org/0000-0001-7104-7816
Matthew W. Griesbach
University of Minnesota
Yun You
University of Minnesota
James R. Dutton
University of Minnesota
Walter C. Low
University of Minnesota
Peter A. Santi
University of Minnesota

Short report

Keywords: Inner ear, Spiral Ganglion Neurons, Neurogenin1, Blastocyst Complementation, Stem Cells, Regenerative Medicine

Posted Date: December 28th, 2020

DOI: https://doi.org/10.21203/rs.3.rs-57441/v2

Version of Record: A version of this preprint was published at Stem Cell Research & Therapy on February 12th, 2021. See the published version at https://doi.org/10.1186/s13287-021-02184-1.

Abstract

This research is the first to produce induced pluripotent stem cell-derived inner ear sensory neurons in the Neurog1 +/- heterozygote mouse using blastocyst complementation. Additionally, this approach corrected non-sensory deficits associated with Neurog1 heterozygosity, indicating that complementation is specific to endogenous Neurog1 function. This work validates the use of blastocyst complementation as a tool to create novel insight into the function of developmental genes and highlights blastocyst complementation as a potential platform for generating chimeric inner ear cell types that can be transplanted into damaged inner ears to improve hearing.

Introduction

Hearing loss is the most common neurosensory deficit. Approximately 488 million individuals world-wide and 15% of Americans have some degree of hearing loss (1). Hearing depends on the mechano-sensory hair cells (HCs) and their innervating neurons, the spiral ganglion neurons (SGNs), which are responsible for transmitting auditory information from the HCs in the organ of Corti to the cochlear nucleus in the brainstem. Mammalian HCs and SGNs do not regenerate after damage, which results in sensorineural hearing loss (SNHL) (2). In addition, auditory neuropathy with relative preservation of hair cells is a substantial cause of deafness (3, 4). Cochlear implants are the only established therapy for severe to profound hearing loss; however, they require a viable SGN population for their success and efficacy (5).

Using exogenous stem cells to replace lost inner ear neurons is a potential strategy if stem cell derived neurons can form central and peripheral connections, form synapses on hair cells and cochlear nucleus neurons, and re-establish functional and tonotopic circuits (6). While, early attempts to target cochlear tissues using stem cells largely produced unremarkable results (6, 7), two promising *in vivo* studies have shown that stem cells can survive and supplement SGNs within a cochlea and even partially restore hearing function (8, 9). However, there are two potential weakness in the previous studies: 1) Since the transplanted stem cells were differentiated *in vitro* to form otic progenitors and due to the lack of using established markers of inner ear specific neurons, these cells may not be equivalent to SGNs formed *in vivo*, which may explain the observed limited functional recovery; and 2) using allogenic stem cells requires that the transplant recipient may need to undergo long-term immunosuppression to prevent rejection of the transplanted progenitors. We address these potential limitations by adopting the technique of blastocyst complementation (BC) to generate inner ear neurons from induced pluripotent stem cells (iPSCs).

BC is a technique in which deletion of a key gene for the development of a specific lineage creates a vacant niche (organogenesis disabled phenotype) that can be complemented by the progeny of wild type pluripotent stem cells injected into embryos at the blastocyst stage of development. Resulting chimeras from BC have successfully generated entire, functional organs, such as the pancreas, kidney, eye, and lung, derived from the progeny of donor stem cells, by complementing genes necessary for their formation (Pancreatic And Duodenal Homeobox1 (PDX1), Sal-Like Like Protein 1 (SALL1), Melanocyte

Inducing Transcription Factor (MITF), and Fibroblast Growth Factor Receptor 2 (FGFR2), respectively (10-15).

These studies, using both intraspecies (mouse X mouse (11, 14) and pig X pig (12)) and interspecies (rat X mouse (10, 13)) chimeras, demonstrated the feasibility of BC to generate organs. Organogenesis is a complex developmental process requiring hierarchical cell and tissue differentiation, coordinated in time and space in response to changes in local and distant signaling cues. Replicating these conditions in vitro to generate functional tissues, let alone organs, has proven extremely challenging and using the embryo to initiate the appropriate signaling cascades is a significant advantage of a BC approach. BC is the only current method for making fully functional, three-dimensional organs from pluripotent cells and generating human organs in large mammalian hosts may be able to address the critical worldwide problem of organ shortages for transplantation (16). However, several hurdles still need to be overcome to make interspecies organ farming a reality (17). For one, all components of an organ will be need to be derived from human tissue, which includes the endothelial, stromal and possibly the immune cells (18-20). While progress has been made on this front (21), it will take time to advance to point of being able to generate entirely whole organs with BC.

By contrast, the replacement of specific cell types could improve health conditions such as pancreatic beta islet cells for Type 1 diabetes (22, 23), dopamine secreting neurons in Parkinson's disease (PD) (24), and inner ear sensory cells for hearing disorders and may be a more readily attainable goal. BC has been used to generate rat islet cells that normalized glucose levels after transplantation into diabetic mice (25), and candidate genes have been identified to create replacement dopaminergic neurons using BC for PD (16); however, BC has not been used to generate sensory cell types in the inner ear. Here we present the first demonstration using intraspecies BC to create mouse donor stem cell-derived inner ear sensory neurons.

Ma and colleagues (26, 27) developed a *Neurogenin1* (*Neurog1*)$^{-/-}$ knockout mouse that lacked an otic ganglion at embryonic day (E)10.5, which translated into postnatal day (P)0 inner ears that lacked afferent, efferent, and autonomic nerve fibers. In preliminary experiments using the *Neurog1*$^{-/-}$ mutant mouse, we produced the first histological analysis of E18.5 *Neurog1*$^{-/-}$ null inner ears (28), which confirmed the findings of Ma and colleagues. With the goal of generating stem cell-derived inner ear neurons, the *Neurog1*$^{-/-}$ knockout animal was the optimal choice for creating a vacant niche to generate inner ear neurons by blastocyst complementation

Methods

All methods performed in this manuscript were in accordance with all policies of the University of Minnesota Institute of Animal Care Use Committee (IACUC), which approved the use and housing of these animals according to accepted principles of laboratory animal care (National Research Council 2003).

Mice

The *Neurog1*$^{tm1And/J}$ mouse strain was used (26, 27) (Jackson Laboratory, Stock No. 017306*)* in which the coding exon for *Neurog1* was replaced with a green fluorescent protein (GFP) cassette fused to a PGK-neo cassette successfully abolishing gene function in *Neurog1*$^{-/-}$ null mice (26-28). Expression of the GFP mRNA was reported to mirror *Neurog1* endogenous gene function which confirmed the specificity of the transgene knock in. However, GFP protein expression was undetectable indicating that the GFP transcript generated in these mice results in a nonfunctional GFP protein (26). Mice were housed in a specific pathogen free (SPF), Research Animal Resource (RAR) and American Association for Accreditation of Laboratory Animal Care, (AAALAC) approved facility, and plastic cages that were steam cleaned and autoclaved 3 times per week. The mouse colony was maintained by crossing *Neurog1*$^{+/+}$ wildtype mice with *Neurog1*$^{+/-}$ heterozygous mice. Experimental mice were generated through heterozygous matings (*Neurog1*$^{+/-}$ X *Neurog1*$^{+/-}$), which produced the following combinations of genotype: *Neurog1*$^{+/+}$ wild-type*, Neurog1*$^{+/-}$ heterozygous*, Neurog1*$^{-/-}$ null mice. *Neurog1*$^{-/-}$ null mice die 24 hours after birth due to their inability to suckle, and were only generated for blastocyst complementation or embryonic harvest. Toe clips were collected at one week of age, which were subsequently hydrolyzed for genotyping analysis. Genotyping was performed by Polymerase Chain Reaction (PCR) using the Jackson Laboratory's validated genotyping protocol: https://www.jax.org/Protocol?stockNumber=017306&protocolID=23926

Genotyping was performed with the following primers: WT Forward (ACCACTAGGCCTTTGTAAGG), Mutant Forward (ATAGACCGAGGGCAGCTTCA), and a Common Reverse primer (CGCTTCCTCGTGCTTTACGGTAT). Genotyping was run in two separate reactions: (1) WT Forward, a sequence which detects endogenous Neurog1 protein, and the Common primer and (2) the Mutant Forward, which is a sequence in the neomycin cassette, and the Common primer. This reaction yields a 198-bp wild type band and a 500-bp mutant band. Wild type animals will have only one wild type band, heterozygotes will have both wild type and mutant bands, and homozygous nulls will only have a mutant band (Supplemental Fig. 1).

Blastocyst Complementation

Mouse x mouse blastocyst complementation was performed by injecting membrane bound GFP-labeled mouse iPSCs into *Neurog1*-deficient blastocysts. The derivation of the 3F10 iPSC line used was previously described in detail by Greder and colleagues (29). Briefly, the iPSCs were derived from Oct4-MerCreMer mTmG mice. These mice are from a cross between Oct4-MerCreMer mice carrying a tamoxifen-inducible Cre knock-in transgene upstream of the 3' UTR of Oct4 (Jackson Laboratory, Stock No: 016829) and a homozygous tdTomato/EGFP reporter mouse strain (mTmG) (Jackson Laboratory, Stock No. 007576). iPSCs were generated according to previous reprogramming protocols (30, 31) and resulting pluripotent iPSCs were cultured with tamoxifen diluted in miPSC growth medium to 100 nM. This strategy results in all donor iPSCs being irreversibly labeled with membrane bound EGFP (Supplemental Fig. 2). Injected blastocysts were transferred to pseudopregnant female surrogates, where they were allowed to develop until the time of natural birth. To produce mutant blastocysts an *in vitro*

approach was used. To do this, the egg donors (*Neurog1*$^{+/-}$ heterozygous female mice) were superovulated (32) at 3-4 weeks of age, by giving CARD HyperOva® (Cosmo Bio, Cat. No. KYD-010-EX-X5) 0.1 ml/mouse, intraperitoneally (*i.p.*), at 17:30 pm (mouse room light:dark cycle: 6:00 – 20:00), followed by Human Chorionic Gonadotropin (HCG) (Sigma-Aldrich Cat. No. C 1063), 5 insulin units (IU)/mouse 47 - 48 hours later. Fresh sperm from a *Neurog1* heterozygous (+/-) male was used for IVF. Fertilized eggs were cultured in home-made modified Human Tubal Fluid (mHTF, a.k.a. high calcium HTF) medium until the blastocysts were formed in ~ 72 hours after IVF and ready for microinjection of iPSCs. Each blastocyst was injected with 10 - 15 iPSCs. After blastocyst injection, mouse blastocysts were transferred into the uteri of pseudopregnant surrogate mice. This entire process was performed on three separate occasions. Variability is expected with embryological development and some of the surrogate dams resorbed all the developing embryos. However, we obtained two viable litters and 13 P0 pups were obtained: 2 *Neurog1*$^{+/+}$ wild type animals, 9 *Neurog1*$^{+/-}$ heterozygote animals, and 2 *Neurog1*$^{-/-}$ homozygote null animals. Of these, one of the wild type samples was highly chimeric, three of the heterozygotes were complemented (30%), and none of the homozygotes exhibited any stem cell derived chimerism.

Inner ear harvesting from the embryo, cyrosectioning, and immunohistochemistry

For tissue harvesting, P1 mice were euthanized using $C0_{2,}$ according to RAR guidelines, followed by decapitation. Heads were bisected with the intention of using one inner ear for cryosectioning and immunohistochemistry (IHC) and the other processed for imaging using scanning Thin Sheet Laser Image Microscope (sTSLIM). Bisected heads were fixed overnight in 4% paraformaldehyde (PFA) in phosphate buffered saline (PBS), and were rinsed with PBS twice for fifteen minutes each before undergoing decalcification in 10% ethylenediaminetetraacetic acid (EDTA) for three days. Inner ears to be analyzed by cryosectioning and IHC were cryoprotected through overnight incubations in ascending concentrations of sucrose up to 30%, and embedded in tissue freezing medium (TFM) (General Data, Cat#: TFM-5) and snap frozen on dry ice. Bisected heads containing the P0 inner ears were sectioned on a cryostat at a thickness of 16mm and directly mounted to slides. The entire ear was collected, starting with sections from the cochlea, through the macular organs, and through the cristae and semicircular canals. Slides were allowed to dry on the slide warmer for a minimum of one hour prior to beginning staining or storing at -20°C. Sectioned tissue was always stained within three days of sectioning. If previously frozen, tissue was rewarmed to room temp by placing on the slide warmer for a minimum of a half hour. Prior to performing immunohistochemistry, epitopes were exposed by performing antigen retrieval. Briefly, slides were placed in Coplin jars filled with boiling sodium citrate buffer with Tween® 20 (Sigma-Aldrich Cat# P9416) (pH adjusted to 6.0 with 1N hydrogen chloride (HCl)) and incubated in a steamer for 20 minutes. Slides were allowed to cool to room temperature, for at least an hour, before continuing the staining protocol. After antigen retrieval, the slides were dried and the sections were outlined with a hydrophobic barrier pen (Super^{HT} Pap Pen, Polysciences Cat# 24230-1). Tissue was rinsed twice (ten minutes each rinse) with PBS and rinsed twice (fifteen minutes each rinse) in PBS with 0.1% Triton™ X-100 (Sigma-Aldrich, X100, Cat# 9002-93-1) (PBST). Non-specific binding was blocked

against using 10% normal horse serum (ThermoFisher, Cat# 16050122) in 0.1% PBST for one hour at room temperature. Primary antibodies, diluted in the blocking solution, were applied and allowed to incubate in the 4°C cold room overnight. All antibodies are listed in the below table. The following day, slides was rinsed with four 15-minute washes in 0.1% PBST, sections were incubated in secondary antibodies, diluted in blocking solution, for two hours at room temperature. The tissue was then rinsed in 0.1% PBST with two ten-minute washes, and counterstained with 4',6-diamidino-2-phenylindole (DAPI, Thermo Fisher Scientific, Cat# D1306) at a concentration of 1:5000 for five minutes. Lastly, tissue was rinsed for ten minutes in PBS, and coverslips were mounted to the slide after applying mounting medium with anti-fade agent (Electron Microscopy Services, Cat# 17985-11). Slides were sealed using with CoverGrip^{TM} Coverslip Sealant (Thermo Fischer Scientific, Cat# NC0154994).

1° Antibodies

Antibody	Vendor	Cat#	Dilution
rabbit polyclonal a-MYO6	Proteus Biosciences Inc.	25-6791	1:500
chicken a-GFP	Abcam Inc.	ab13970	1:1000
mouse monoclonal a-Tuj1	Biolegend	MMS-435P	1:1000

2° Antibodies

Antibody	Vendor	Cat#	Dilution
488 donkey a-chicken	Jackson ImmunoResearch Alexa Fluor	703-545-155	1:1000
555 donkey a-rabbit	Invitrogen Alexa Fluor	Ab150062	1:1000
647 donkey a-mouse	Invitrogen Alexa Fluor	A-31571	1:1000

Microscopy and Image processing·

All immunohistochemical imaging was performed on a Leica inverted light microscope. Images were exported as raw Leica Image File Format (LIF) files and processed in FIJI (Fiji Is Just ImageJ). The resolution of each image was adjusted to 300 dots per inch, which reflects pixels per inch (DPI) in Photoshop, and all resulting JPEGs were assembled using Adobe Illustrator.

sTSLIM macro light-sheet microscope

In 2008 we developed a high-resolution microtome/microscope called scanning Thin Sheet Laser Image Microscope (sTSLIM) that can image whole cochleas, nondestructively (33-37). sTSLIM optically

sections and digitizes all cochlear tissues to allows for a complete quantitative assessment of normal and pathological structures. The Santi laboratory has used sTSLIM to characterize mouse cochlear development (38), analyze normal spiral ganglion cell number in the mouse (39), and illustrate alterations in cochlear structures in two knock-out mouse models (Atonal homolog1, ATOH1 and N-Myc proto-oncogene protein, N-Myc) (40, 41). Since light scatter and absorption are the greatest limiting factors in resolution, we have performed both tissue engineering (improved transparency and accessibility to antibody labeling through decellularization) and optical engineering (scanned light-sheet, Bessel beam illumination, structured illumination, confocal line detection, and radial sectioning) to improve imaging of large specimens such as the mouse cochlea with portions of the brain attached. Microscope performance will be tested on a regular basis using 150 nm gold fluorescent beads to ensure that the point spread function of the microscope is stable and optimal for reproducible imaging.

Tissue preparation for sTSLIM

Inner ears processed for sTSLIM were fixed and decalcified (described above) and then underwent a dehydration series in ascending concentrations of ethanol (30%, 50%, 70%, 100% EtOH) and then lightly stained by Rhodamine-B isothiocyante (5mg/mL in 100%) for 1 hour. After rinsing in 100% EtOH, inner ears were cleared to transparency with BABB (benzyl alcohol: benzyl benzoate 1:2), and specimens were mounted to a specimen rod and placed in a BABB-filled chamber for imaging by sTSLIM.

sTSLIM imaging

sTSLIM optically sections non-destructively by moving a thin light sheet in the X- and Z-axes. A z-stack of well-aligned 2D optical sections of the inner ear was automatically imaged with x-axis scanning across the width of the specimen and with a z-step size of 5 µm. At this thickness the whole mouse cochleae contained ~300 images that take ~30 minutes to produce. Images were adjusted for brightness, contrast, and either unsharp masking or deconvolution using ImageJ (National Institutes of Health). The z-stack was then loaded into the Amira 3D program and structures of interest were manually segmented, by drawing along their borders in different colors to prepare 3D reconstructions and volume calculations. Supplemental Fig. 3 shows an example of a 2D optical section through the cochlea and Supplemental Movie 1 shows segmented inner ears rotating horizontally.

Results

Donor GFP-labeled stem cells create chimeric spiral ganglion and vestibular neurons in the *Neurog1*$^{+/-}$ heterozygote

Neurog1-deficient blastocysts were established by performing *in vitro* fertilization (IVF) with zygotes extracted from *Neurog1*$^{+/-}$ heterozygous dams and fresh sperm from *Neurog1*$^{+/-}$ heterozygous male mice. Blastocysts were injected with EGFP-labeled mouse induced pluripotent stem cells (iPSCs) at approximately embryonic day (E)3.5 and subsequently were transferred into surrogate pseudopregnant dams **(Fig. 1A)**. The iPSCs were derived from transgenic mice that carried a tamoxifen-inducible CreER

transgene under the control of the *Oct4* promoter and a Cre-dependent tdTomato / EGFP reporter cassette. The iPSCs used in this study were from cells previously cultured with tamoxifen to activate the Oct4 driven CreER, removing the tdTomato reporter gene and activating EGFP expression. As Oct4 is highly expressed in iPSCs this strategy irreversibly labels all the donor stem cells and their progeny with EGFP **(Supplemental Fig. 2)**. Upon analysis of chimeric inner ears at P1, robust and specific incorporation of GFP-labled cells derived from the donor stem cells was seen in the SGN of a *Neurog1*$^{+/-}$ heterozygote (**Fig. 1)**.

In the complemented *Neurog1*$^{+/-}$, GFP-labeled iPSCs contributed to the SGN and descending neuronal processes in the cochlea with minimal donor stem cell-derived cell incorporation in other tissue (**Fig. 1D,E arrowheads**). The specificity of labeling in the *Neurog1*$^{+/-}$ was unmistakable, given the lack of GFP labeling observed in the wild type SGN (**Fig. 1C,F, arrows**). Progeny of the GFP-labeled donor iPSCs also contributed to the cell bodies of Scarpa's ganglion (**Fig. 1G**), in addition to vestibular neurons innervating the cristae ampullaris (**Fig. 1H,I**). Since *Neurog1* is known to be required for the formation of both cochlear and vestibular neurons (27), these results indicate that the integration pattern of cells derived from the wild type donor cells recapitulates that expected from cells with wild type endogenous *Neurog1* gene function and that *Neurog1* haplodeficiency creates a vacent niche that can be filled by cells derived from exogenous stem cells to produce SGNs using BC.

Complementation of *Neurog1*-deficiency is distinct from general chimerism

A chimera is defined as a composite animal comprised of two genetically distinct cell populations (42). Performing BC in wild type animals will result in random chimerization throughout the developing embryo (43, 44). When performing BC in knockout blastocysts, in addition to exogenous donor-derived cells targeting a vacant developmental niche, random chimerism can also be observed in non-targeted cell types.

Two examples of complemented *Neurog1*$^{+/-}$ heterozygotes were highly chimeric, as a high degree of specific donor-derived cell integration into the SGN was observed (**Fig. 2B-D'**), in addition to general chimerism, which was evident from the widespread GFP expression in non-sensory otic cell types (**Fig. 2B-D'**). This general chimerism is similar to that observed in the *Neurog1*$^{+/+}$ control, which also displayed the incorporation of GFP-expressing cells in non-sensory cells. Notably, the *Neurog1*$^{+/-}$ heterozygote SGNs, in some regions, appeared to be derived nearly entirely from donor iPSCs, whereas the *Neurog1*$^{+/+}$ wild type SGNs were consistently negative for GFP expression (**Figs. 1C, 2A,A'**).

The extent of donor-derived cell chimerism in the *Neurog1*$^{+/+}$ wild type in comparison to the complemented *Neurog1*$^{+/-}$ heterozygotes was assessed further by looking at the resepective level of GFP expression in the temporal lobe of the brain. This analysis clearly showed the incorporation of exogenous iPSC-derived cells in the *Neurog1*$^{+/+}$ brain at a comparable level to the complemented *Neurog1*$^{+/-}$ heterozygotes (**Fig. 2E,F**). Therefore, chimeras successfully formed regardless of geneotype, but in the absence of a *Neurog1*-deficient niche, GFP-expressing cells derived from the exogenous donor iPSCs

could not contribute to the formation of the SGN in wild type inner ears (**Figs. 1F, 2A'**). These results support our hypothesis by demonstrating that BC can specifically generate SGNs using WT donor stem cells.

We did not see complementation in the two *Neurog1*$^{-/-}$ mutant embryos that we obtained. However, both nulls showed few to no GFP-expressing cells engrafted throughout the whole embryo, suggesting that the lack of complementation was due to low chimerism. With an increased sample size, we expect to obtain highly chimeric *Neurog1*$^{-/-}$ mutants in which all of the SGNs are derived from donor stem cell progeny. Therefore, it is anticipated that, following Mendel's law, 75% of blastocysts (heterozygous and null) obtained from BC will give rise to chimeric inner ears.

Donor stem cells extensively contibute to the complemented *Neurog1*$^{+/-}$ vestibule

In the highly chimeric complemented *Neurog1*$^{+/-}$ inner ears, the contribution of donor-derived GFP-labeled cells appeared to increase in sections through the more basal cochlea in a trend that was dramatically more evident in the vestibule. In fact, it appeared that the majority of cells in the vestibule were derived from donor iPSCs, given the extensive presence of GFP in all vestibular cell types. Specifically, GFP entirely co-expressed with the neuronal marker class III beta-tubulin (TUJ1) in the neurites innervating the vestibular sensory organs **(Fig 3A-B', arrow head and dotted lines),** in addition to many Myosin 6 (MYO6)-expressing vestibular hair cells (**Fig 3A-B, red**) and non-sensory cells **(Fig 3A'-B', small arrows)**. While the degree of donor cell contribution to the complemented *Neurog1+/-* vestibule was striking, the biological significance of this was lacking, until a clear heterozygote effect in non-complemented *Neurog1*$^{+/-}$ inner ears was detected.

Blastocyst complementation rescues *Neurog1*$^{+/-}$ inner ear malformations

Non-complemented *Neurog1*$^{+/-}$ heterozygote inner ears were observed to have inner ear morphological non-sensory malformations, which included inner ears reduced in size by approximately 60% of the wildtype control (**Fig 4A, Supplemental Movie 1**). Three-dimensional reconstructions revealed overt malformations particularly in the vestibule, in which the anterior and lateral ampullae and the saccule were notably reduced in size **(Fig. 4A-D, Supplemental Movie 1).** This finding was confirmed via cryosections, which displayed that the non-complemented *Neurog1*$^{+/-}$ vestibule sometimes had an abnormally orientated saccule, utricle, and anterior ampullae. Specifically, unlike the typical orthogonal arrangement of the utricular and saccular maculae observed in the wild type vestibule, the non-complemented *Neurog1*$^{+/-}$ sensory maculae (denoted by MYO6-expressing hair cells) were oriented in parallel (**Fig. 4E,F; red, small arrows**). Additionally, the utricular maculae and anterior crista ampullaris were unusually close to one another (**Fig. 4F**, **arrowheads**). Moreover, in some cases, the lateral ampulla appeared connected to the lateral semi circular canal (**Fig. 4I, arrowheads**). Impaired non-sensory vestibular morphology was observed in four of the six *Neurog1*$^{+/-}$ heterozygotes obtained and analyzed. Strikingly, the remaining two *Neurog1*$^{+/-}$ heterozygotes completely lacked a vestibule (not shown).

Together these observations suggest that a reduction in non-sensory cell formation and/or a failure of sensory organ separation occured with the reduction of *Neurog1* gene dose.

Cochlear and vestibular HCs developed normally in the *Neurog1*$^{+/-}$ heterozygote (as has been reported for the *Neurog1*$^{-/-}$ mutant) despite impaired non-sensory formation. However, sensory development potentially occurred at the expense of non-sensory development, as ectopic HCs were sometimes seen in non-sensory regions in the lateral semi circular canal (**Fig. 4I'**).

Importantly, non-sensory defects observed in the *Neurog1*$^{+/-}$ heterozygotes were rescued in complemented *Neurog1*$^{+/-}$ samples (**Fig. 4A'-D,G,J)**. Given the extensive contribution of GFP to non-sensory tissue in the complemented *Neurog1*$^{+/-}$ heterozygous vestibular sensory organs **(Fig. 3)**, these results suggest that widespread incorporation of cells derived from the donor iPSCs to the vestibule in the complemented *Neurog1*$^{+/-}$ heterozygote is not random, but rather reflects the recovery of a previously unappreciated biological function of *Neurog1* in inner ear morphogenesis. This finding demonstrates the use of BC as a tool to elucidate novel gene function and to confirm or disprove concepts regarding the development of neurobiological systems.

Discussion

Presented here for, the first time, is the intraspecies complementation of *Neurog1*-deficient mouse blastocysts to generate a chimeric population of donor iPSC-derived SGNs. This is a major advancement in the field of regenerative medicine for hearing disorders. The complexity of the intersecting developmental pathways involved in lineage specification of inner ear sensory cells is a difficult task to recapitulate *in vitro* (6). By contrast, following blastocyst complementation, the developing embryo initiates these processes to produce what are presumed to be authentic spiral ganglion neurons. The approach of using BC to target *Neurog1*-deficiency is also advantageous, as *Neurog1* is well-characterized to specify inner ear neuroblasts during the otocyst stage, a developmental stage when the future inner ear is a simple structure on a cellular level (45-47). Therefore, it would be a straightforward workflow to **1.)** use blastocyst complementation to target a *Neurog1*-deficient niche in order to generate chimeric otocysts, that can **2.)** be surgically extracted, **3.)** GFP-labeled neuroblasts derived from donor cells isolated by flow cytometry, and **4.)** could be transplanted to inner ears with damaged neuronal innervation. The prospect of isolating and transplanting autologous BC-derived cells has been successfully demonstrated when pancreatic islet cells were extracted from mouse-rat chimeras and transplanted into a chemically-induced mouse diabetes model and normalized host blood glucose levels for over a year (25). Moreover, developing the therapeutic application for using BC to create inner ear neurosensory cells is simpler than the goal of using BC for the generation of entire organs, which may require the nullification of several genes, such as those required for development of the vasculature system (48) in order to prevent immune rejection.

Many outstanding hurdles exist in the BC field, which includes matching the developmental timing between the host blastocyst and donor cells of different species, which is a particular challenge for

creating chimeras with human tissue. However, great strides have been made in better understanding the optimal cellular status in PSCs (naïve vs primed) necessary for successfully creating interspecies chimeras, in addition to ways of promoting survival of the donor cells (49-54). Therefore, these barriers seem likely to be overcome, as indicated by the creation of successful human-animal chimeras (55, 56).

Using iPSCs for BC was designed to circumvent ethical issues associated with using embryonic stem cells (ESCs) and with the goal of creating autologous organs/tissues for transplantion to avoid immune rejection by the recipient. While a number of studies support this conclusion by showing that transplanted derivatives of pluripotent stem cells do not evoke an immune response (57, 58), a few recent studies have raised concerns (59) that include potential immunogenicity of iPSCs. Specifically it has been found that human induced pluripotent stem cells (hiPSCs) can sometimes be rejected by allogeneic and autologous natural killer cells (NK) (60) and cells derived from iPSCs can similarly activate the immune system (19). Due to these mixed results, caution will be warranted when moving interspecies BC into the transplantation arena. However, safer alternatives to immunosuppressants are being developed. Since rejection is primarily mediated by T cell-dependent recognition of foreign antigens (61), strategies such as modulation of the T cell costimulatory and inhibitory pathways are being developed to safely protect the iPSCs-derived transplants from immune rejection (62, 63). Other approaches to providing immune protection for transplants are by targeted disruption of the activation of antigen presenting cells. For instance, blocking the expression of the major histocompatibility complex (MHC) class II transactivator in human embryonic stem cells (hESCs) leads to the silencing of HLA class II expression and thereby making these cells immune evasive. Therefore, there will likely be feasible options for developing safe and effective strategies to support iPSCs-based regenerative medicine in the near future.

Unlike other studies using BC, we demonstrated that simply being haplodeficient for a master fate determining gene is sufficient to generate BC derived tissue, which adds nuance to the complementation field. This unexpected finding led to the analysis of heterozygous inner ears with and without complementation and generated data that suggests that *Neurog1* is dose-dependently required for non-sensory development while largely preserving neurosensory development. This may suggest that *Neurog1* is involved in a binary decision to either adopt a non-sensory or neurosensory fate through an interaction with Notch signaling, a notion consistent with previous studies (26, 45, 46, 64). Importantly, the observed non-sensory defects in the *Neurog1*$^{+/-}$ were rescued in successfully complemented chimeric samples **(Fig 4)**. This supports the idea that our complementation results cannot be attributable to general chimerism, but rather are specific to an endogenous role for *Neurog1* in inner ear morphogenesis in addition to neurogenesis. *Neurog1* has been previously fate mapped in non-sensory regions of the cochlea and maculae (46), therefore this work provides evidence of a functional role for *Neurog1* in these areas and supports the likelihood of *Neurog1* playing additional roles in inner ear development beyond simply promoting inner ear neurogenesis

Here we establish, using intraspecies mouse chimeras, that BC is a platform that can be used for generating inner ear cell types. The generation of hiPSCs enables generation of tissues that are either autologous or from closely related genetic background as the recipient (65). Therefore, this work sets the

stage for interspecies complementation with the goal of generating human inner ear tissues using swine as biological incubators, which could lead to improved research models and drug screening methodologies and ultimately transplantation to deaf patients to improve hearing.

Abbreviations

AA: anterior ampulla

AAALAC: American association for accreditation of laboratory animal care

ATOH1: atonal homolog 1

ASCC: anterior semicircular canal

BABB: benzyl alcohol: benzyl benzoate

BC: blastocyst complementation

E: embryonic day

EDTA: ethylenediaminetetraacetic acid

ESCs: embryonic stem cells
DAPI: 4',6-diamidino-2-phenylindole

DPI: dot per inch (which reflects pixels per inch)

FGFR2: fibroblast growth factor receptor 2

FIJI: Fiji Is Just ImageJ

GFP: green fluorescent protein

hESCs: human embryonic stem cells

HC: hair cell

HCl: hydrogen chloride

HCG: human chorionic gonadotropin

hiPSCs: human induced pluripotent cells

HTF/mHTF: human tubal fluid and modified human tubal fluid

IACUC: institute of animal care use committee

***i.p.*:** intraperitoneally

iPSCs: induced pluripotent stem cell

IHC: immunohistochemistry

LA: lateral ampulla

LIF: Leica image file format

LSCC: lateral semicircular canal

MHC: major histocompatibility complex

MITF: melanocyte inducing transcription factor

MYO6: unconventional myosin VI

Neurog1: *Neurogenin1*

N-Myc : N-Myc proto-oncogene protein

P: postnatal day

PA: posterior ampulla

PBS: phosphate buffered saline

PBST: phosphate buffered saline with 0.1% Triton X-100

PCR: polymerase chain reaction

PD: Parkinson's disease

PDX1: pancreatic and duodenal homeobox1

PFA: paraformaldehyde

PSCC: posterior semicircular canal

RAR: research animal resources

RC: Rosenthal's Canal with SGNs

SAC: saccule

SALL1: Sal-like like protein 1

SGNs: spiral ganglion neurons, the auditory nerve

SPF: specific pathogen free

SNHL: sensorineural hearing loss

sTSLIM: scanning thin sheet laser image microscope

TFM: tissue freezing medium

TUJ1: class III beta-tubulin

Ut: utricle

VG: vestibular ganglion

Declarations

Ethics approval and consent to participate

Not applicable.

Consent for publication

Not applicable.

Availability of data and materials

Data sharing is not applicable to this article as no datasets were generated or analyzed during the current study.

Author contributions: A.S. carried out the immunohistochemical studies, microscopy analysis, prepared figures, and drafted the manuscript. A.S and M.G. performed the genotyping. A.S. and M.G. harvested and processed inner ear tissue for analysis. M.G. participated in the mouse colony management and the sTSLIM analysis. Y.Y. performed the blastocyst complementation and embryo transfers. J.D. created the EGFP-labeled induced pluripotent stem cell line. W.L. and P.S. conceived of the study. A.S., W.L, and P.S. participated in the experimental design. W.L., P.S., and A.S. provided resources. A.S., J.D., W.L., and P.S. revised the paper. All authors read and approved the final manuscript.

Competing interests

The authors declare no financial or competing interests.

Funding

Research reported in this publication was supported by the National Institute on Deafness and Other Communication Disorders of the National Institutes of Health under award number F31DC015153 (Predoctoral Fellowship, ARS) and the National Institute on Aging of the National Institute of Health under award number 2T32AG029796-11 (Postdoctoral Fellowship, ARS), and a private donation from Bridget Sperl and John McCormick supported the development of the *Neurog1*$^{-/-}$ mice and the acquisition of resources (PAS and WCL). The content is solely the responsibility of the authors and does not necessarily represent the official views of the National Institutes of Health.

Acknowledgements

We would like to acknowledge individuals from the University of Rochester, in Rochester NY, Dr. Amy Kiernan, Dr. Patricia White, Dr. J. Christopher Holt, and Dr. Lin Gan, who provided expert mentorship and training of A.S., which supported the development of this project. Additionally, we would like to acknowledge members of the Stem Cell Institute at the University of Minnesota for advice and support.

References

1. WHO. Deafness and hearing loss 2019 [Available from: https://www.who.int/news-room/fact-sheets/detail/deafness-and-hearing-loss.
2. Yamasoba T, Lin FR, Someya S, Kashio A, Sakamoto T, Kondo K. Current concepts in age-related hearing loss: epidemiology and mechanistic pathways. Hear Res. 2013;303:30-8.
3. Uus K, Bamford J. Effectiveness of population-based newborn hearing screening in England: ages of interventions and profile of cases. Pediatrics. 2006;117(5):e887-93.
4. Starr A, Picton TW, Sininger Y, Hood LJ, Berlin CI. Auditory neuropathy. Brain. 1996;119 (Pt 3):741-53.
5. Bradley J, Beale T, Graham J, Bell M. Variable long-term outcomes from cochlear implantation in children with hypoplastic auditory nerves. Cochlear Implants Int. 2008;9(1):34-60.
6. Nayagam BA, Edge, A.S. Stem Cells for the Replacement of Auditory Neurons. In: Dabdoub AF, B.; Popper, A.N.; Fay, R.R., editor. The Primary Auditory Neurons of the Mammalian Cochlea: Springer, New York, NY; 2016. p. 263 -86.
7. Ito J, Kojima K, Kawaguchi S. Survival of neural stem cells in the cochlea. Acta Otolaryngol. 2001;121(2):140-2.
8. Chen W, Jongkamonwiwat N, Abbas L, Eshtan SJ, Johnson SL, Kuhn S, et al. Restoration of auditory evoked responses by human ES-cell-derived otic progenitors. Nature. 2012;490(7419):278-82.
9. Corrales CE, Pan L, Li H, Liberman MC, Heller S, Edge AS. Engraftment and differentiation of embryonic stem cell-derived neural progenitor cells in the cochlear nerve trunk: growth of processes into the organ of Corti. J Neurobiol. 2006;66(13):1489-500.
10. Kobayashi T, Yamaguchi T, Hamanaka S, Kato-Itoh M, Yamazaki Y, Ibata M, et al. Generation of rat pancreas in mouse by interspecific blastocyst injection of pluripotent stem cells. Cell. 2010;142(5):787-99.

11. Usui J, Kobayashi T, Yamaguchi T, Knisely AS, Nishinakamura R, Nakauchi H. Generation of kidney from pluripotent stem cells via blastocyst complementation. Am J Pathol. 2012;180(6):2417-26.
12. Matsunari H, Nagashima H, Watanabe M, Umeyama K, Nakano K, Nagaya M, et al. Blastocyst complementation generates exogenic pancreas in vivo in apancreatic cloned pigs. Proc Natl Acad Sci U S A. 2013;110(12):4557-62.
13. Goto T, Hara H, Sanbo M, Masaki H, Sato H, Yamaguchi T, et al. Generation of pluripotent stem cell-derived mouse kidneys in Sall1-targeted anephric rats. Nat Commun. 2019;10(1):451.
14. Mori M, Furuhashi K, Danielsson JA, Hirata Y, Kakiuchi M, Lin CS, et al. Generation of functional lungs via conditional blastocyst complementation using pluripotent stem cells. Nat Med. 2019;25(11):1691-8.
15. Zhang H, Huang J, Li Z, Qin G, Zhang N, Hai T, et al. Rescuing ocular development in an anophthalmic pig by blastocyst complementation. EMBO Mol Med. 2018;10(12).
16. Crane AT, Aravalli RN, Asakura A, Grande AW, Krishna VD, Carlson DF, et al. Interspecies Organogenesis for Human Transplantation. Cell Transplant. 2019;28(9-10):1091-105.
17. Suchy F, Nakauchi H. Interspecies chimeras. Curr Opin Genet Dev. 2018;52:36-41.
18. Freedman BS. Hopes and Difficulties for Blastocyst Complementation. Nephron. 2018;138(1):42-7.
19. Zhao T, Zhang ZN, Rong Z, Xu Y. Immunogenicity of induced pluripotent stem cells. Nature. 2011;474(7350):212-5.
20. Liu X, Li W, Fu X, Xu Y. The Immunogenicity and Immune Tolerance of Pluripotent Stem Cell Derivatives. Front Immunol. 2017;8:645.
21. Hamanaka S, Umino A, Sato H, Hayama T, Yanagida A, Mizuno N, et al. Generation of Vascular Endothelial Cells and Hematopoietic Cells by Blastocyst Complementation. Stem Cell Reports. 2018;11(4):988-97.
22. Najarian JS, Sutherland DE, Matas AJ, Steffes MW, Simmons RL, Goetz FC. Human islet transplantation: a preliminary report. Transplant Proc. 1977;9(1):233-6.
23. Agarwal A, Brayman KL. Update on islet cell transplantation for type 1 diabetes. Semin Intervent Radiol. 2012;29(2):90-8.
24. Grealish S, Diguet E, Kirkeby A, Mattsson B, Heuer A, Bramoulle Y, et al. Human ESC-derived dopamine neurons show similar preclinical efficacy and potency to fetal neurons when grafted in a rat model of Parkinson's disease. Cell Stem Cell. 2014;15(5):653-65.
25. Yamaguchi T, Sato H, Kato-Itoh M, Goto T, Hara H, Sanbo M, et al. Interspecies organogenesis generates autologous functional islets. Nature. 2017;542(7640):191-6.
26. Ma Q, Chen Z, del Barco Barrantes I, de la Pompa JL, Anderson DJ. neurogenin1 is essential for the determination of neuronal precursors for proximal cranial sensory ganglia. Neuron. 1998;20(3):469-82.
27. Ma Q, Anderson DJ, Fritzsch B. Neurogenin 1 null mutant ears develop fewer, morphologically normal hair cells in smaller sensory epithelia devoid of innervation. J Assoc Res Otolaryngol. 2000;1(2):129-

43.
28. Steevens AR, Glatzer JC, Kellogg CC, Low WC, Santi PA, Kiernan AE. SOX2 is required for inner ear growth and cochlear nonsensory formation prior to sensory development. Development. 2019.
29. Greder LV, Gupta S, Li S, Abedin MJ, Sajini A, Segal Y, et al. Analysis of endogenous Oct4 activation during induced pluripotent stem cell reprogramming using an inducible Oct4 lineage label. Stem Cells. 2012;30(11):2596-601.
30. Takahashi K, Yamanaka S. Induction of pluripotent stem cells from mouse embryonic and adult fibroblast cultures by defined factors. Cell. 2006;126(4):663-76.
31. Morita S, Kojima T, Kitamura T. Plat-E: an efficient and stable system for transient packaging of retroviruses. Gene Ther. 2000;7(12):1063-6.
32. Takeo T, Nakagata N. Superovulation using the combined administration of inhibin antiserum and equine chorionic gonadotropin increases the number of ovulated oocytes in C57BL/6 female mice. PLoS One. 2015;10(5):e0128330.
33. Schroter TJ, Johnson SB, John K, Santi PA. Scanning thin-sheet laser imaging microscopy (sTSLIM) with structured illumination and HiLo background rejection. Biomed Opt Express. 2012;3(1):170-7.
34. Santi PA, Johnson SB, Hillenbrand M, GrandPre PZ, Glass TJ, Leger JR. Thin-sheet laser imaging microscopy for optical sectioning of thick tissues. Biotechniques. 2009;46(4):287-94.
35. Schacht P, Johnson SB, Santi PA. Implementation of a continuous scanning procedure and a line scan camera for thin-sheet laser imaging microscopy. Biomed Opt Express. 2010;1(2):598-609.
36. Buytaert JA, Johnson SB, Dierick M, Salih WH, Santi PA. MicroCT versus sTSLIM 3D imaging of the mouse cochlea. J Histochem Cytochem. 2013;61(5):382-95.
37. Santi PA. Light sheet fluorescence microscopy: a review. J Histochem Cytochem. 2011;59(2):129-
38. Kopecky B, Johnson S, Schmitz H, Santi P, Fritzsch B. Scanning thin-sheet laser imaging microscopy elucidates details on mouse ear development. Dev Dyn. 2012;241(3):465-80.
39. Johnson SB, Schmitz HM, Santi PA. TSLIM imaging and a morphometric analysis of the mouse spiral ganglion. Hear Res. 2011;278(1-2):34-42.
40. Kopecky BJ, Duncan JS, Elliott KL, Fritzsch B. Three-dimensional reconstructions from optical sections of thick mouse inner ears using confocal microscopy. J Microsc. 2012;248(3):292-8.
41. Pan N, Jahan I, Kersigo J, Kopecky B, Santi P, Johnson S, et al. Conditional deletion of Atoh1 using Pax2-Cre results in viable mice without differentiated cochlear hair cells that have lost most of the organ of Corti. Hear Res. 2011;275(1-2):66-80.
42. McLaren A. Mammalian Chimeras: Cambridge University Press; 1976.
43. Wu J, Platero-Luengo A, Sakurai M, Sugawara A, Gil MA, Yamauchi T, et al. Interspecies Chimerism with Mammalian Pluripotent Stem Cells. Cell. 2017;168(3):473-86 e15.
44. Xiang AP, Mao FF, Li WQ, Park D, Ma BF, Wang T, et al. Extensive contribution of embryonic stem cells to the development of an evolutionarily divergent host. Hum Mol Genet. 2008;17(1):27-37.

45. Abello G, Khatri S, Giraldez F, Alsina B. Early regionalization of the otic placode and its regulation by the Notch signaling pathway. Mech Dev. 2007;124(7-8):631-45.
46. Raft S, Koundakjian EJ, Quinones H, Jayasena CS, Goodrich LV, Johnson JE, et al. Cross-regulation of Ngn1 and Math1 coordinates the production of neurons and sensory hair cells during inner ear development. Development. 2007;134(24):4405-15.
47. Steevens AR, Sookiasian DL, Glatzer JC, Kiernan AE. SOX2 is required for inner ear neurogenesis. Sci Rep. 2017;7(1):4086.
48. Wang X, Shi H, Zhou J, Zou Q, Zhang Q, Gou S, et al. Generation of rat blood vasculature and hematopoietic cells in rat-mouse chimeras by blastocyst complementation. J Genet Genomics. 2020.
49. Theunissen TW, Friedli M, He Y, Planet E, O'Neil RC, Markoulaki S, et al. Molecular Criteria for Defining the Naive Human Pluripotent State. Cell Stem Cell. 2016;19(4):502-15.
50. Gafni O, Weinberger L, Mansour AA, Manor YS, Chomsky E, Ben-Yosef D, et al. Derivation of novel human ground state naive pluripotent stem cells. Nature. 2013;504(7479):282-6.
51. Wang X, Li T, Cui T, Yu D, Liu C, Jiang L, et al. Human embryonic stem cells contribute to embryonic and extraembryonic lineages in mouse embryos upon inhibition of apoptosis. Cell Res. 2018;28(1):126-9.
52. Huang K, Zhu Y, Ma Y, Zhao B, Fan N, Li Y, et al. BMI1 enables interspecies chimerism with human pluripotent stem cells. Nat Commun. 2018;9(1):4649.
53. Masaki H, Kato-Itoh M, Takahashi Y, Umino A, Sato H, Ito K, et al. Inhibition of Apoptosis Overcomes Stage-Related Compatibility Barriers to Chimera Formation in Mouse Embryos. Cell Stem Cell. 2016;19(5):587-92.
54. Wu J, Okamura D, Li M, Suzuki K, Luo C, Ma L, et al. An alternative pluripotent state confers interspecies chimaeric competency. Nature. 2015;521(7552):316-21.
55. James D, Noggle SA, Swigut T, Brivanlou AH. Contribution of human embryonic stem cells to mouse blastocysts. Dev Biol. 2006;295(1):90-102.
56. Mascetti VL, Pedersen RA. Human-Mouse Chimerism Validates Human Stem Cell Pluripotency. Cell Stem Cell. 2016;18(1):67-72.
57. de Almeida PE, Meyer EH, Kooreman NG, Diecke S, Dey D, Sanchez-Freire V, et al. Transplanted terminally differentiated induced pluripotent stem cells are accepted by immune mechanisms similar to self-tolerance. Nat Commun. 2014;5:3903.
58. Guha P, Morgan JW, Mostoslavsky G, Rodrigues NP, Boyd AS. Lack of immune response to differentiated cells derived from syngeneic induced pluripotent stem cells. Cell Stem Cell. 2013;12(4):407-12.
59. Yoshihara M, Hayashizaki Y, Murakawa Y. Genomic Instability of iPSCs: Challenges Towards Their Clinical Applications. Stem Cell Rev Rep. 2017;13(1):7-16.
60. Kruse V, Hamann C, Monecke S, Cyganek L, Elsner L, Hubscher D, et al. Human Induced Pluripotent Stem Cells Are Targets for Allogeneic and Autologous Natural Killer (NK) Cells and Killing Is Partly

Mediated by the Activating NK Receptor DNAM-1. PLoS One. 2015;10(5):e0125544.
61. Benichou G, Gonzalez B, Marino J, Ayasoufi K, Valujskikh A. Role of Memory T Cells in Allograft Rejection and Tolerance. Front Immunol. 2017;8:170.
62. Rong Z, Wang M, Hu Z, Stradner M, Zhu S, Kong H, et al. An effective approach to prevent immune rejection of human ESC-derived allografts. Cell Stem Cell. 2014;14(1):121-30.
63. Szot GL, Yadav M, Lang J, Kroon E, Kerr J, Kadoya K, et al. Tolerance induction and reversal of diabetes in mice transplanted with human embryonic stem cell-derived pancreatic endoderm. Cell Stem Cell. 2015;16(2):148-57.
64. Mann ZF, Galvez H, Pedreno D, Chen Z, Chrysostomou E, Zak M, et al. Shaping of inner ear sensory organs through antagonistic interactions between Notch signalling and Lmx1a. Elife. 2017;6.
65. Park IH, Zhao R, West JA, Yabuuchi A, Huo H, Ince TA, et al. Reprogramming of human somatic cells to pluripotency with defined factors. Nature. 2008;451(7175):141-6.

Figures

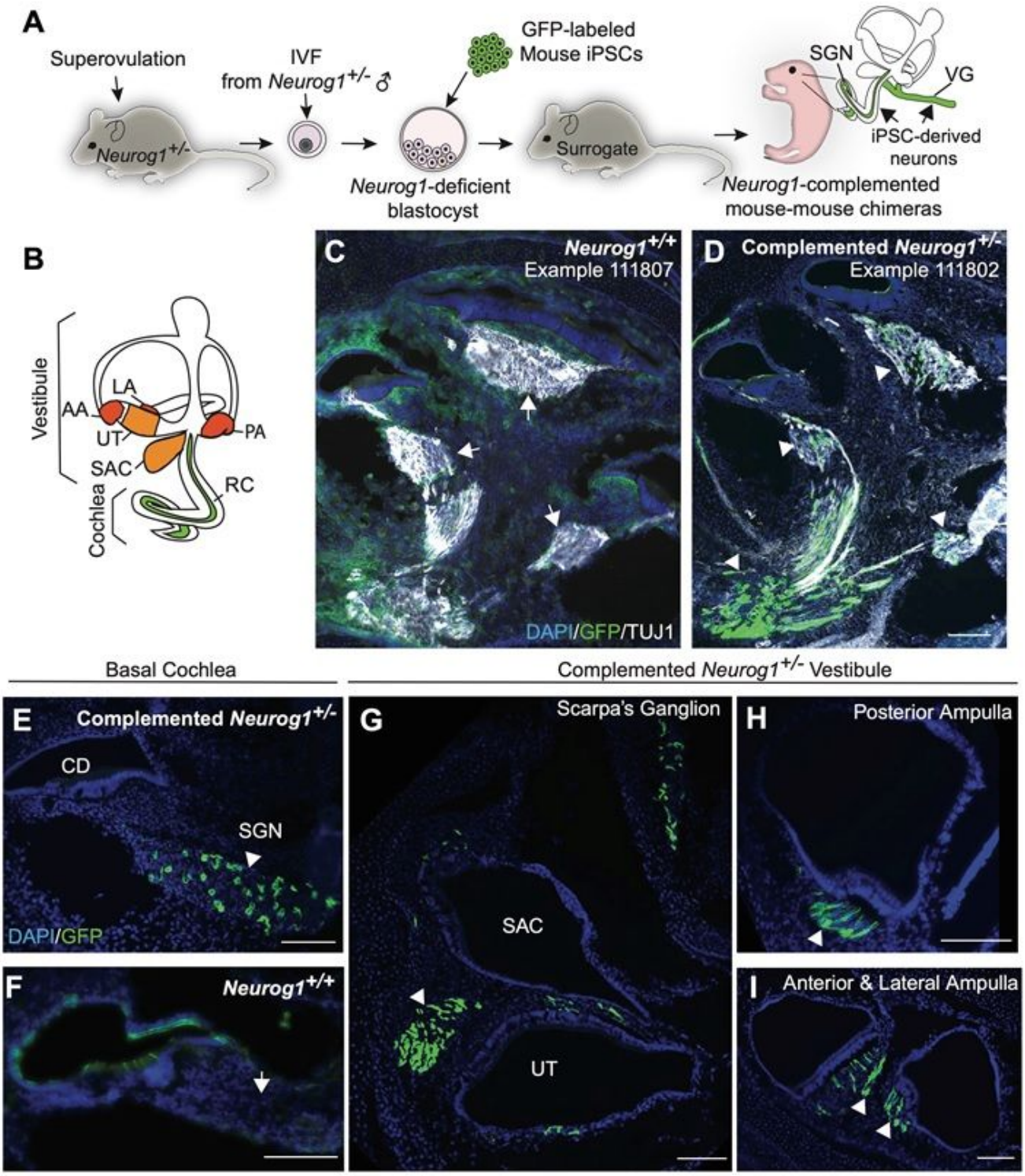

Figure 1

Donor GFP-labeled stem cells create chimeric spiral ganglion and vestibular neurons in the Neurog1 heterozygote (A) Schematic of experimental methods for BC. Neurog1+/- female mice were superoverulated with hormones. Zygotes were extracted and fertilized by in vitro fertilization (IVF) with Neurog1+/- male sperm and allowed to mature until blastocyst stage (~E3.5), at which point all blastocysts were injected with GFP-labeled iPSCs. Complemented blastocysts were transferred to a

pseudopregnant surrogate. Pregnancies were to taken to birth, embryos were harvested, and complementation in the inner ear was assessed. (B) Diagram of the inner ear indicates the vestibular (balance) portion and cochlear (auditory) portion. Low magnification of the midmodiolar region of the cochlea in (C) representative image of the Neurog1+/+ wild type inner ear shows the absence of GFP-labeled stem cells in the SGN (arrows) (Images are from a single Neurog1+/+ wild type (1/2), sample number 111807) in contrast to (D) specific stem cell complementation in the SGN in a Neurog1+/- heterozygote (arrowheads) (Images are from a single complemented Neurog1+/- heterozygote (1/3), sample number 111802). High magnification images of the basal cochlear turn show (E) the presence of GFP-labeled stem cells in a Neurog1+/- heterozygote SGN (arrowhead) and absence in (F) the Neurog1+/+ wild type SGN (arrow). Specific stem cell complementation was seen in the vestibule of a Neurog1+/- heterozygote, (G) in Scarpa's ganglion adjacent to the utricle (UT) and saccule (Sac), (H) neurites (arrowhead) innervating the posterior ampulla, and (I) neurites innervating the anterior and lateral ampullae (arrowheads). AA: Anterior Ampulla, LA: Lateral Ampulla, PA: Posterior Ampulla, Ut: Utricle, SAC: Saccule, RC: Rosenthal's Canal with SGNs. All scale bars are 100mm. Scale bar in D also corresponds to C.

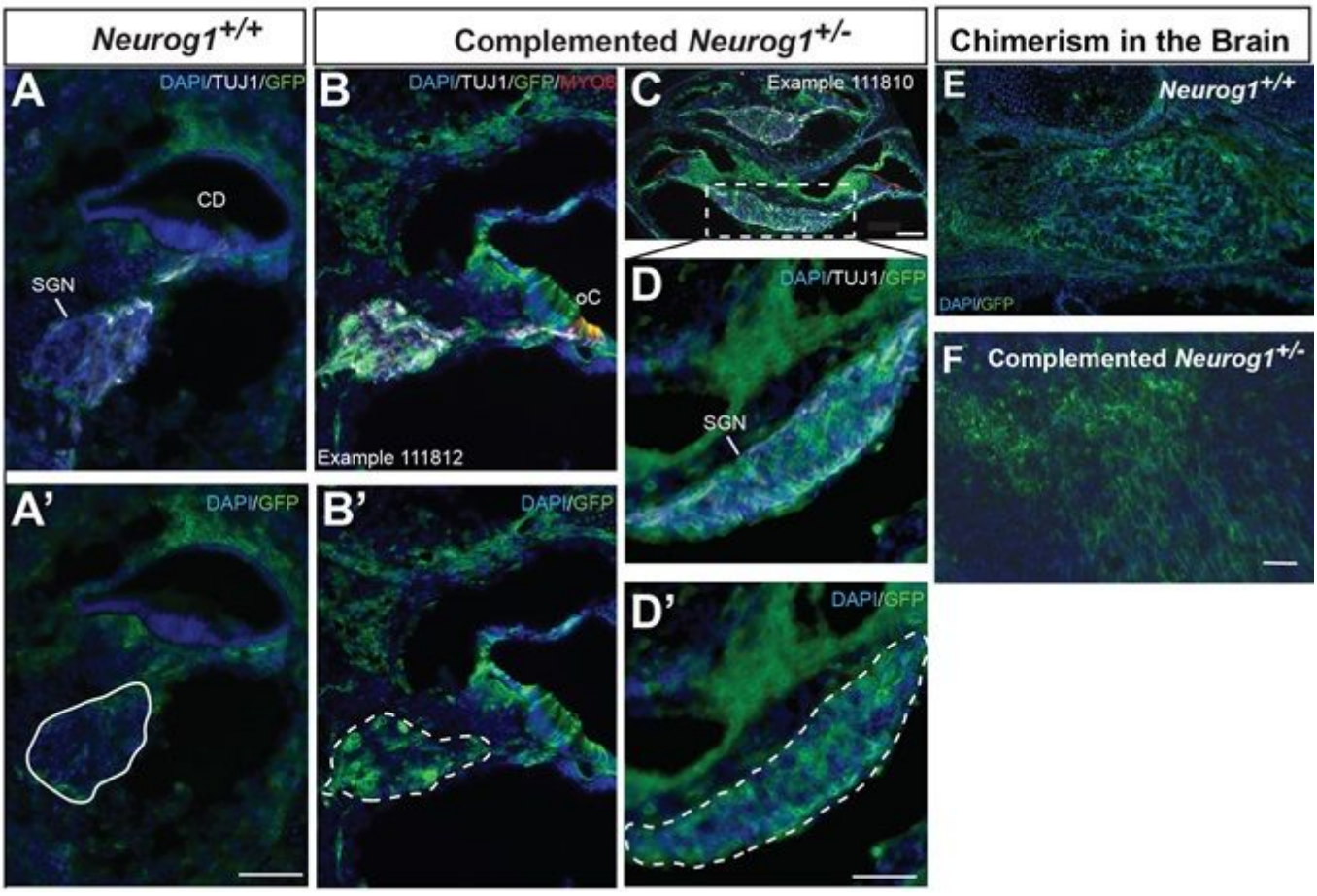

Figure 2

Complementation of Neurog1-deficiency is distinct from general chimerism. (A,A') High magnification of the basal turn in a chimeric Neurog1+/+cochlea does not show the engraftment of iPSCs in the spiral ganglia, (solid outline) compared to (B-D') examples from two separate chimeric and complemented

Neurog1+/- cochleas in which iPSCs extensively contribute to the SGN (dotted outline). Chimerism was seen in both the (E) Neurog1+/+ brain and (F) the Neurog1+/- brain, indicating that while both embryos successfully formed chimeras, donor cells did not specifically contribute to the SGN in the absence of a vacant niche. (Images are from a single Neurog1+/+ wild type (1/2), sample number 111807 and two separate complemented heterozygotes (2/3) sample numbers 111812 and 111810) All scale bars are 100mm. Scale bar in A' corresponds to A-B', scale bar in F corresponds to E. DAPI: 4,6-diamidino-2-phenylindole, TUJ1: class III beta-tubulin antibody, GFP: green fluorescent protein antibody against endogenous fluorescence, MYO6: Unconventional Myosin VI antibody.

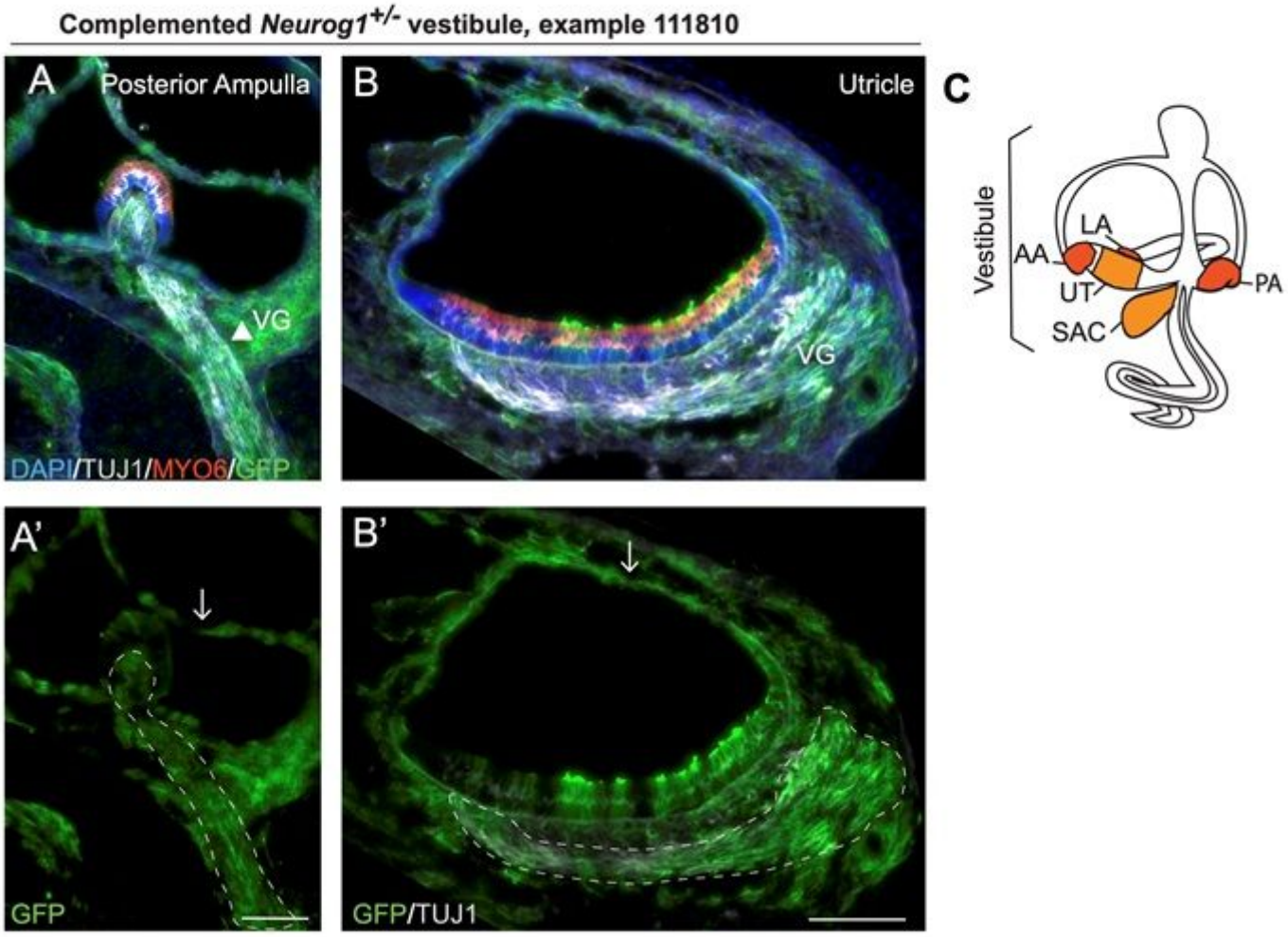

Figure 3

Donor stem cells extensively contibute to a complemented Neurog1+/- vestibule. High magnification of the (A,A') posterior ampulla and (B,B') utricle in a highly chimeric complemented Neurog1+/- vestibule shows that GFP-labeled donor iPSCs contribute to the near entirely of both structures (n=1, sample number 111810). GFP co-expresses with TUJ1-labeled vestibular nerves in the vestibular ganglia (VG) (dotted outlines), some MYO6-labeled vestibular hair cells (red), and non-sensory vestibular tissue (white arrows) (C) Inner ear diagram shows the anatomy of the vestibule with anterior ampulla (AA), lateral

ampulla (LA), posterior ampulla (PA), saccule (SAC) and utricle (UT). VG: vestibular ganglion. All scales bars are 100mm.

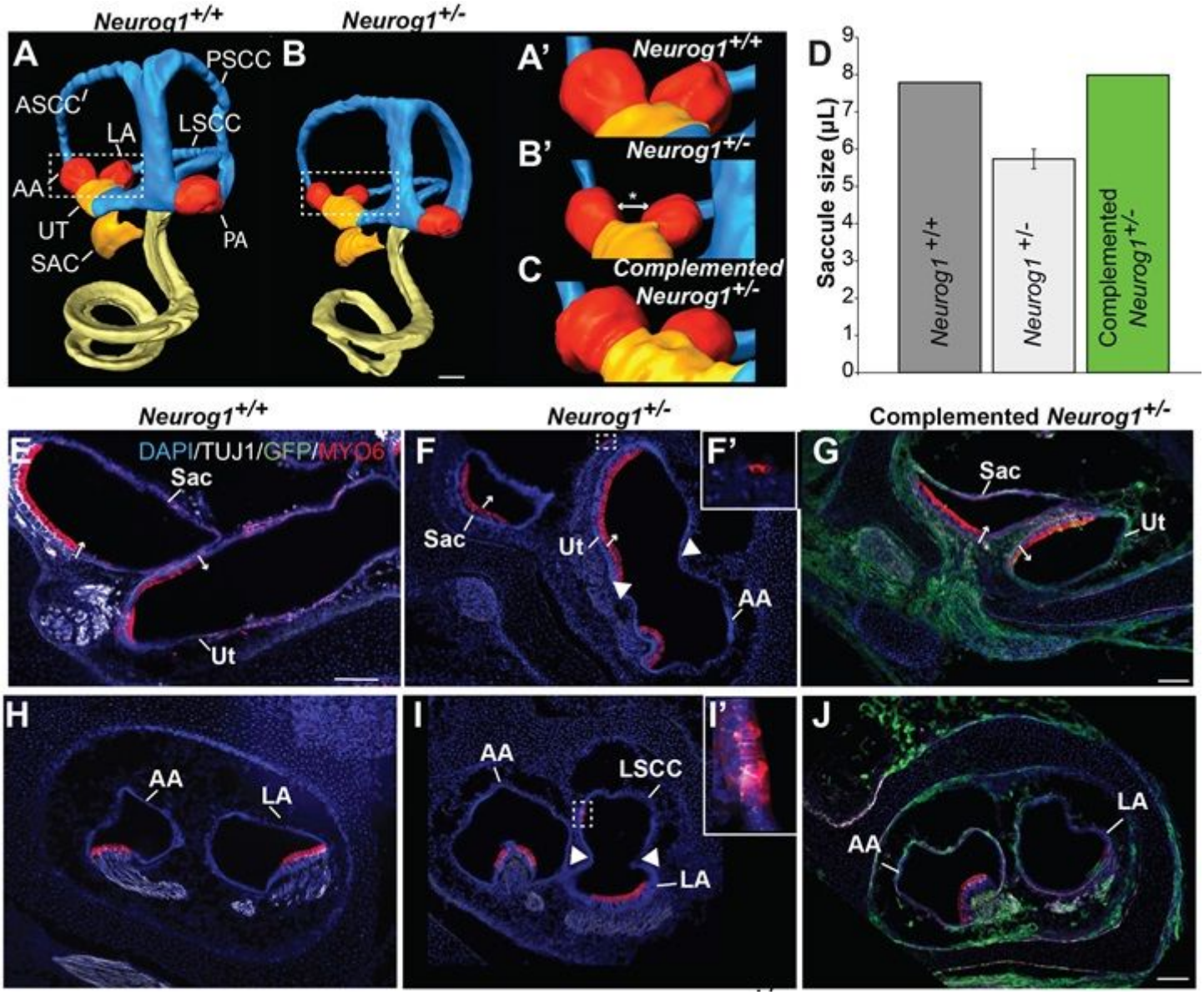

Figure 4

The Neurog1+/- heterozygous vestibule showed non-sensory defects that were rescued by stem cell complementation. Three-dimensional reconstructions of (A) a Neurog1+/+ wild type inner ear compared to (B) a Neurog1+/- inner ear, reveals a marked size and morphological difference between genotypes, which is particularly noticeable in the anterior (AA) and lateral ampullae (LA) (dotted boxes). (A',B') Higher magnification images of the dotted boxes from A and B and (C) a comparable region from a complemented Neurog1+/- heterozygote, shows a rescue of vestibular morphogenesis (D) Quantification of utricular volume in a Neurog1+/+ (n=2), non-complemented Neurog1+/- (n=3), and a complemented Neurog1+/- heterozygote (n=1) shows the rescue of the non-complemented Neurog1+/- utricular size with donor stem cell complementation. (E) Cross-section through the saccule (SAC) and utricle (UT) in a Neurog1+/+ control shows the characteristic orthogonal orientation of the sensory maculae that is

reflected in the perpendicular orientation of the sensory hair cells in each organ (small arrows). By contrast, (F) the Neurog1+/- heterozygous vestibule had a smaller saccule (SAC) and utricle (UT) and the hair cells in the sensory maculae were orientated in the same direction (small arrows, red). Additionally, the Neurog1+/- heterozygous anterior ampulla (AA) was unusually close to the utricle (arrowheads) (n=4). (F') Ectopic hair cells were occasionally seen in the Neurog1+/- heterozygous vestibular ganglia adjacent to the vestibule. These non-sensory and sensory defects were rescued in (G) complemented Neurog1+/- heterozygote samples (n=3). Similarly, compared to (H) the anterior (AA) and lateral ampullae (LA) in a Neurog1+/+ control, (I) the non-complemented Neurog1+/- heterozygous anterior ampullae (AA) was smaller and appeared connected to the lateral semi-circular canal (LSCC, arrowheads). (I') Ectopic hair cells were sometimes seen in the semicircular canals (box). These defects were rescued in (J) complemented Neurog1+/- samples. All scale bars are 100μm. Scale bar in B also corresponds to A; scale bar in G corresponds to E and F; scale bar in J corresponds to H & I.

Supplementary Files

This is a list of supplementary files associated with this preprint. Click to download.

- hetwtcomparisonimovie.mp4
- SupplementalMaterials.pdf